

TUNABLE LASER SPECTROMETERS FOR SPACE SCIENCE. C. R. Webster¹, L. E. Christensen¹, G. J. Flesch¹, S. Forouhar¹, R. Briggs¹, D. Keymeulen¹, J. Blacksberg¹ and P. R. Mahaffy², ¹Jet Propulsion Laboratory, California Institute of Technology, 4800 Oak Grove Drive, Pasadena, CA 91109; Chris.R.Webster@jpl.nasa.gov ²NASA Goddard Space Flight Center (GSFC), 8800 Greenbelt Rd., Greenbelt, Md., 20771. Paul.R.Mahaffy@nasa.gov

Introduction: Tunable laser spectrometers have enjoyed a huge growth in capability for a wide range of applications in scientific research, medicine, industry, Earth and planetary space missions. Miniaturization of instruments resulting from development of room-temperature laser devices has enabled the development of powerful new instruments for space science: for planetary missions to planets, satellites and primitive bodies; for the International Space Station (ISS) cabin monitoring; and for In Situ Resource Utilization (ISRU) including for the Mars 2020 mission.

Room Temperature Infrared Laser Development: The first atmospheric measurements were made in the 1980's [1] using the newly invented lead-salt tunable diode lasers that required liquid helium cooling and produced only a few microwatts of output power, and then in several modes (wavelengths). The BLISS high-altitude balloon instrument weighed 1,500 kg and a single laser package (cryostat) weighed 70 kg. By the 1990's when liquid-nitrogen cooled lasers were available, several groups [2] from all over the world were flying tunable laser spectrometers on a wide variety of aircraft to understand Earth's ozone hole chemistry and dynamics. In the early 2000's with Quantum Cascade (QC) lasers available, the transition to room temperature operation began in earnest [3], so that by 2005 miniature laser spectrometers were being considered for planetary missions such as the Mars Science Laboratory (MSL) mission.

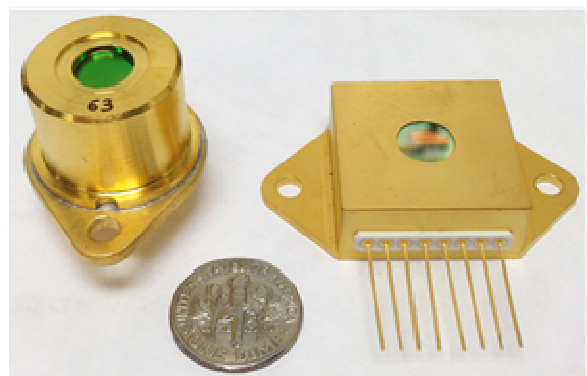


Fig. 1. QC lasers (with integrated TEC's) for sensing OCS and CO on Venus, developed at JPL's Microdevices Lab (MDL) at 4.82 μm with either built-in single lens collimator (left) or without (right). Output powers of >10 mW at 25°C are typical for these devices.

Today, room temperature QC (Fig.1), Interband Cascade (IC) and tunable diode lasers are available [4] over a large wavelength region, accessing molecules of interest to planetary science not just at the shorter near-IR wavelengths but also accessing mid-IR wavelengths (Fig. 2) from HF (2.3 μm) to NH₃ (10 μm).

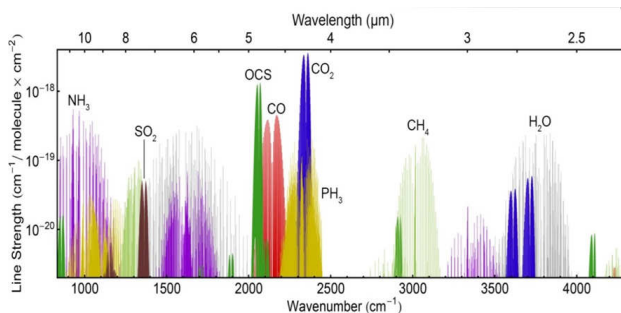


Fig. 2. IR bands of species of interest to planetary science, in particular for Venus, Saturn and Uranus probe missions.

IR Tunable Laser Spectroscopy: Tunable laser spectrometers are uniquely suited to making high-precision gas abundance and stable isotope ratios because of their ability to scan at ultra-high resolution (0.0001 cm^{-1}) over targeted individual rovibrational spectral lines of the gas of interest without interferences that can be of concern with mass spectrometers.

For light molecules at pressures below ~ 100 mbar, IR tunable laser spectroscopy offers a direct, non-invasive, unambiguous method for measuring stable isotope ratios to sensitivities of $\sim 1\%$ for planetary low-mass (<5 kg), all-solid-state instruments. Tunable laser spectrometers are well suited to H₂O, NO, NO₂, HNO₃, O₃, CO, CO₂, NH₃, SO₂, HCl, N₂O and CH₄.

Success for this method lies in the spectroscopy of the IR region (1-30 μm), in which most simple molecules have several vibrational bands (3N-6 for non-linear, 3N-5 for linear molecules) containing ~ 100 rotational absorption lines from which key lines can be chosen that are well separated and without interference. High symmetry in simple molecules like tetrahedral CH₄ can produce degeneracies and a complex rovibrational line system, but linewidths for most molecules are typically <0.02 cm^{-1} . With a laser linewidth $1/20^{\text{th}}$ of the molecular linewidth, high sensitivity is achieved since there is no significant "instrument func-

tion” to broaden measured lines and thereby reduce absorption depths.

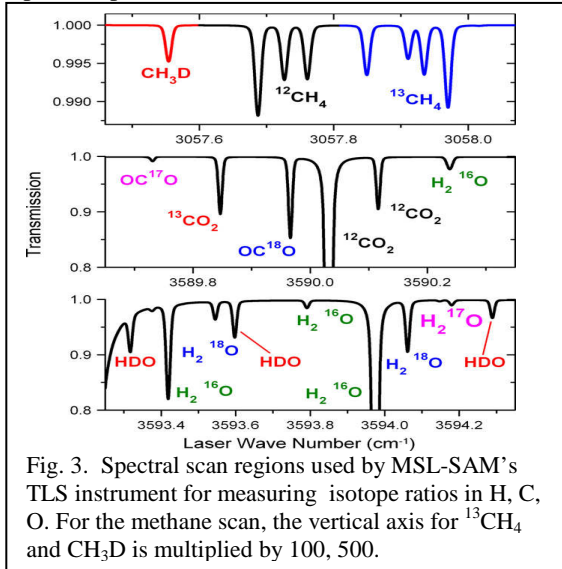


Fig. 3. Spectral scan regions used by MSL-SAM’s TLS instrument for measuring isotope ratios in H, C, O. For the methane scan, the vertical axis for $^{13}\text{CH}_4$ and CH_3D is multiplied by 100, 500.

Isotopic shifts between vibrational bands depend to a first order on reduced mass differences; for HDO and H_2O this is large, while for ^{13}C this is more typically about 11 cm^{-1} (but varies). In methane at $3.3\text{ }\mu\text{m}$, we are fortunate that the 11-cm^{-1} shift does not dump the $^{13}\text{CH}_4$ line group on top of the adjacent $^{12}\text{CH}_4$ group but to the side (see Fig. 3).

Unlike mass spectrometers, laser spectrometers are not dependent on the mass ratio dynamic range, but can be tuned to regions where both parent and minor isotope (e.g. $^{12}\text{CO}_2$ and $^{13}\text{CO}_2$ and/or ^{18}OCO) have absorption lines of similar intensity (see Fig. 8), improving precision. Because CO_2 and H_2O have numerous overlapping bands, this is readily done, a luxury not afforded to the isolated CH_4 band at $3.3\text{ }\mu\text{m}$, and we are stuck with $^{13}\text{CH}_4$ lines that are typically ~ 90 times weaker than those of $^{12}\text{CH}_4$.

Stable Isotope Ratios: Stable isotope ratios in C, H, N, O and S are powerful indicators of a wide variety of planetary geophysical processes that can identify origin, transport, temperature history, radiation exposure, atmospheric escape, environmental habitability and biology [5]. For the Allan Hills 84001 meteorite, for example, the $^{13}\text{C}/^{12}\text{C}$ ratio identifies it as a Mars (SNC) meteorite; the $^{40}\text{K}/^{40}\text{Ar}$ ratio tells us the last time the rock cooled to solid, namely 4 Gya; isotope ratios in ^3He , ^{21}Ne and ^{38}Ar show it was in space (cosmic ray exposure) for 10-20 million years; ^{14}C dating that it sat in Antarctica for 13,000 years before discovery; and clumped isotope analysis of $^{18}\text{O}^{13}\text{C}^{16}\text{O}$ in its carbonate that it was formed at $18\pm 4\text{ }^\circ\text{C}$ in a near-surface aqueous environment [6].

Isotopic ratios offer the key to unraveling the complex dynamics and chemistry associated with the for-

mation and evolution of planetary bodies (planets, satellites and primitive bodies) including differentiation by retaining a fingerprint record of temperature, radiation environment and sun-distance location through equilibrium, disequilibrium, and variety of temperature-dependent chemical processes. For stable isotope ratios in 3-isotope systems, departures from mass-dependent (MD) fractionation have detailed a variety of processes from ozone hole photochemistry (O) to the emergence of life (S) and planetary migrations (O).

Carbon $^{13}\text{C}/^{12}\text{C}$ isotope ratio. Biological processes are well known to prefer the use of ^{12}C (evaporation, diffusion through leaf stomata, enzyme reactions) and produce depletions in $\delta\text{-}^{13}\text{C}$ that are typically 2.7% for C_3 plants that use Calvin-Benson photosynthesis pathway, and 1.3% for C_4 plants using the Hatch-Slack pathway [7]. This fractionation has been used in climate change studies to identify sources and sinks of the increasing atmospheric carbon dioxide since its $\delta\text{-}^{13}\text{C}$ values distinguish oceanic and biospheric sources.

Oxygen isotope ratios. In the triple isotope plot (Fig. 4) of $\delta\text{-}^{17}\text{O}$ vs. $\delta\text{-}^{18}\text{O}$ [8], lunar samples fall on the mass-dependent (slope = 0.5) terrestrial fractionation line, evidence used that the Moon formed during the final stages of Earth’s accretion 4.5 Gya when Earth collided with another large body (Theia) originating from the same region of the solar nebula [9]. While some meteoritic classes join Earth, Moon and Mars in slopes of 0.5 (although with different offsets and therefore reservoirs), at the big picture of Fig. 6, most solar system bodies (solar oxygen, chondrules, molecular clouds and asteroidal water) lie on the unity mass-independent slope. The enrichment in ^{16}O of the Sun measured by Genesis and of calcium-aluminum inclusions (CAI) cannot be reconciled with conventional MD fractionation, and a variety of explanations have been put forward (e.g. supernova injection, CO self-shielding, fractionation in the protoplanetary disk, and even heterogenous chemistry on interstellar dust) [see the review of Dominguez, 2010 [8].

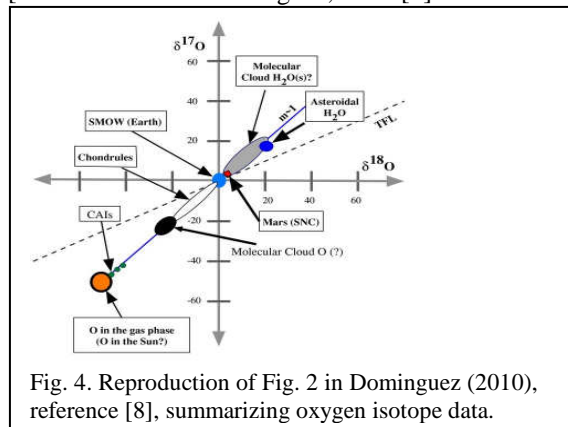


Fig. 4. Reproduction of Fig. 2 in Dominguez (2010), reference [8], summarizing oxygen isotope data.

Clumped isotopes in C and O. As a further constraint on the environment of alteration processes, John Eiler's group developed a method of clumped isotope analysis of $^{18}\text{O}^{13}\text{C}^{16}\text{O}$ in carbonates to identify temperature of formation, used to suggest that carbonates in Allan Hills 84001 were formed at $18 \pm 4^\circ\text{C}$ in a near-surface aqueous environment [6].

Sulfur $^{34}\text{S}/^{33}\text{S}/^{32}\text{S}$ isotope ratios. In triple isotope plots, the " Δ " value is used to quantify the difference (offset) of a delta-value from the mass-dependent slope, which for delta- ^{33}S vs. delta- ^{34}S would be a slope of 0.5. Isotope ratios in S are very powerful for identifying sources and sinks for atmospheric sulfur, and especially photochemical processes (e.g Earth and Venus sulfur cycles), and on Earth played a pivotal role in recording the emergence of life some 2.2 Gya: In the absence of O_2 , stratospheric UV photolysis of SO_2 rained out surface sulfates with a large range of $\Delta^{33}\text{S}$ values, but once cyanobacteria became the main source of surface sulfates, the observed spread was very narrow [10].

Nitrogen $^{15}\text{N}/^{14}\text{N}$ isotope ratio. Planetary atmospheric escape processes depend principally on mass differences, and like $^{13}\text{C}/^{12}\text{C}$, D/H and $^{18}\text{O}/^{16}\text{O}$, the nitrogen $^{15}\text{N}/^{14}\text{N}$ ratio shows enrichment in the atmosphere of Mars. Nitrogen is also very important as a potential biomarker, and as a discriminator in the very different physics of fractionation of molecular nitrogen N_2 and ammonia NH_3 , the latter being a significant component of the ice giants. Unlike water, the sublimation of ammonia ice into vapor and N_2 gas results in little or no isotope exchange in nitrogen [11]. Thus, in conjunction with D/H in water, the $^{15}\text{N}/^{14}\text{N}$ ratio is a powerful discriminator of transport across the "snow" lines of water and ammonia [11].

The D/H Ratio. The D/H ratio exhibits a wide range of enrichments and depletions compared with isotopic (SMOW) standards for two reasons: first, adding a neutron to a light element has a larger effect than doing so to heavier elements like C, N, O, S; second, water undergoes large fractionations during freezing or sublimation due to the large differences in ground state vibrational energy between HDO and H_2O .

On Earth, in partnership with delta- ^{18}O measurements, the D/H ratio has been used to successfully record rainfall maps, detail cirrus cloud formation [12], identify water salinity, and record the long-term climate record [13]. For our solar system, D/H is a powerful tool for identifying origin, transport and evolution. Until the recent observation of Hartley-2 by Hartog et al. [14] from the Herschel Space Observatory, the theory that comets delivered water to Earth was questionable since Oort cloud comets had D/H values three times that of terrestrial SMOW. With the right

D/H ratio, Jupiter-family comets look more likely delivery agents (see Fig. 5).

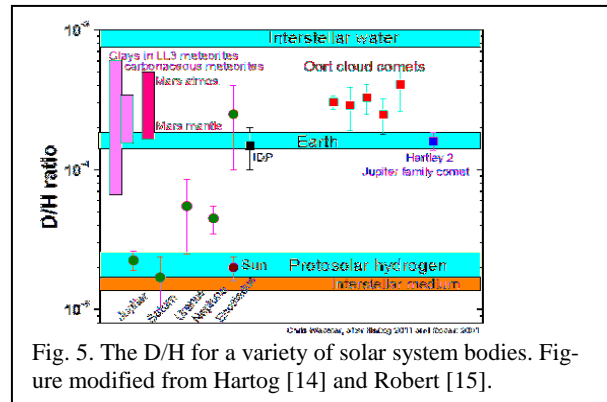


Fig. 5. The D/H for a variety of solar system bodies. Figure modified from Hartog [14] and Robert [15].

TLS in SAM on MSL's Curiosity Rover: The Tunable Laser Spectrometer (TLS) is one of three instruments (Fig. 6) that make up the Sample Analysis at Mars (SAM) suite [16] on the Curiosity rover. In addition to atmospheric measurements, TLS analyzes the gases evolved from pyrolyzing or combusting rock samples acquired by Curiosity.

During its' first two years in operation, TLS has determined the abundance of methane on Mars [17] and its variability at the Gale crater region, as will be updated during the workshop. In addition, both TLS and SAM's Quadrupole Mass Spectrometer (QMS) have measured atmospheric isotope ratios (see table with references [18, 19, 20, 21]) at unprecedented precision that in comparison with meteoritic data, tell a story of prolonged atmospheric escape that has been ongoing for nearly 4 billion years.

TLS has also been looking at the C, O and H isotope ratios in gases evolved from heating rock samples taken from Rocknest [22], John Klein, and Cumberland samples. One important result [23] is measurement by TLS of the D/H in clays from Yellowknife bay, and simultaneous measurement of the D/H in the same sample by the QMS. The low value of the measured D/H indicates that the mudstone was created long before much of the atmospheric escape occurred.

TLS for Venus, Saturn, Titan and Uranus Probes:

In combination with the QMS, TLS is currently on strawman payloads for Discovery and New Frontiers missions that include atmospheric probes, for example for Venus, Saturn [24], Titan [25] and Uranus. In these applications in which a probe is descending very fast through the upper atmosphere, TLS will be upgraded with fast, agile digital electronics that drive several lasers simultaneously to maximize the data quality and return during these short but very important

missions. Target gases include CO, OCS, H₂O, CO₂, SO₂, NH₃ and PH₃ (Fig. 2) and a variety of important isotope ratios. Requirements are typically 1-2% for D/H, and 1 ‰ for the triples isotopes in O and in S.

Table 1. Published results from SAM-MSL on isotope ratios of gases in the Martian atmosphere.

Isotopes	Mars value	Instrument	Reference
$\delta^{38}\text{Ar}$	$310 \pm 31 \text{ ‰}$	QMS	Atreya et al. (2013, <i>GRL in press</i>)
$\delta^{40}\text{Ar}$	$5,419 \pm 1013 \text{ ‰}$	QMS	Mahaffy et al. (2013, <i>Science</i>)
$\delta^{13}\text{C}_{\text{VPDB}}$	$45 \pm 12 \text{ ‰}$	QMS	" "
$\delta^{15}\text{N}$	$572 \pm 82 \text{ ‰}$	QMS	Wong et al. (2013, <i>GRL in press</i>)
δD	$5,880 \pm 60 \text{ ‰}$	TLS	Webster et al. (2013, <i>Science</i>)
$\delta^{13}\text{C}_{\text{VPDB}}$	$46 \pm 4 \text{ ‰}$	TLS	" "
$\delta^{18}\text{O}_{\text{SMOW}}$	$48 \pm 5 \text{ ‰}$	TLS	" "
$\delta^{17}\text{O}_{\text{SMOW}}$	$24 \pm 5 \text{ ‰}$	TLS	" "
$\delta^{13}\text{C}\delta^{18}\text{O}$	$109 \pm 31 \text{ ‰}$	TLS	" "

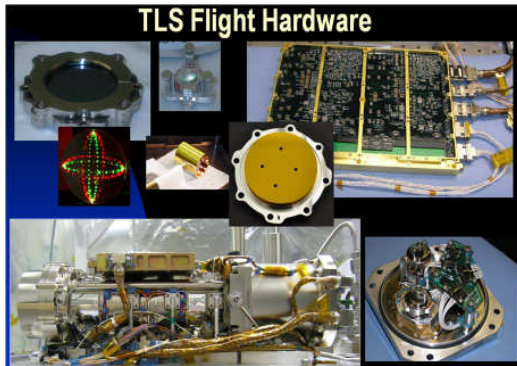


Fig. 6. Photographs of TLS flight hardware as implemented on SAM-MSL. The complete spectrometer is shown in the lower left panel.

TLS as a Combustion Monitor for ISS and on Mars 2020 for In Situ Resource Utilization: In addition to developing TLS for future planetary missions, JPL is building a 5-channel TLS for the International Space Station (ISS) that will serve as a cabin monitor, providing detection of CO, HCN, HF, HCl, and CO₂ as an early warning system of possible fire hazards (Fig. 7). For this application, NASA requires improved accuracy, response time and especially maintainability over existing electrochemical sensors.

Finally, the recent announcement of the payload instruments for Mars 2020 included an experiment aimed at demonstrating in situ resource utilization (ISRU) on Mars; namely the Mars Oxygen ISRU Experiment (MOXIE) instrument (PI Dr. Michael Hecht of MIT) that will be built at JPL. This instrument will produce O₂ and CO from CO₂, and use tunable diode lasers from JPL's Microdevices Lab (MDL) to monitor CO and CO₂ during the conversion process.

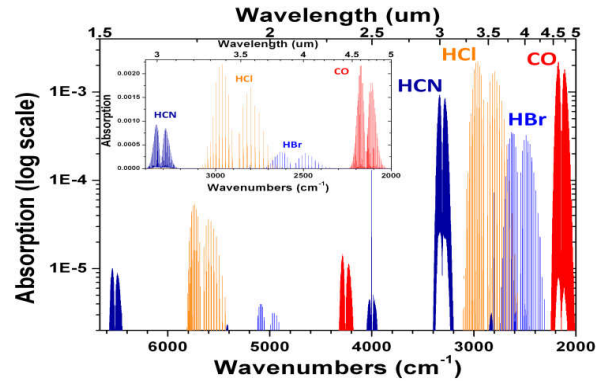


Fig. 7. Absorption wavelengths of bands of relevance to fire detection (Briggs, Forouhar).

References: [1] Webster C.R. and R.D. May, *J. Geophys. Res.* **92**, 11931-11950 (1987). [2] Webster C.R. et al., *Science* **261**, 1130-1134 (1993). [3] Webster C.R. et al., *Applied Optics*, **40**, 321-326, 2001. [4] Forouhar S. et al., *Appl. Phys. Lett.* **105** 051110 (2014) doi: 10.1063/1.4892655 [5] Criss R.E. (1999) *Principles of Stable Isotope Composition*, Oxford University Press, ISBN 0195117751; [6] Halevy L., Fischer W., Eiler J. (2011), doi: 10.1073/pnas.1109444108. [7] O'Leary M. H. (1988). *BioScience* **38** (5): 328–336. DOI: 10.2307/1310735. [8] Dominguez G. (2010) *ApJ* **713** L59 doi:10.1088/2041-8205/713/1/L59. [9] Wiechert, U. et al. (2001), *Science* **294** (12): 345–348. [10] Farquhar J. et al. (2000), *Science* **289**, 756. [11] Owen, T., Bar-Nun, A. (1998) *Farad. Discuss. No. 109*, 453-462. [12] Webster C.R. and Heymsfield A.J. (2003), *Science*, **302**, 1742-1745. [13] Thompson L.G. et al. (2003), *Climatic Change* **59**, 137-155. [14] Hartog P. et al. (2011), *Nature*, doi: 10.1038/nature10519. [15] Robert F. (2001), *Science* **293**, 1056-1058. [16] P. R. Mahaffy, et al., *Space Science Rev.* **170**, 401 (2012). [17] C. R. Webster et al., *Science* **342**, 355 (2013). [18] S. Atreya et al. [19] Mahaffy P.R. et al., doi: 10.1126/science.1237966, *Science* **341**, 263 (2013) [20] Wong et al., *Geophys. Res. Lett.*; [21] C. R. Webster, et al., *Science* **341**, 260 (2013). [22] L. Leshin et al., *Science* **341**, (2013) DOI: 10.1126/Science.1238937. [23] P.R. Mahaffy et al., "The Deuterium to Hydrogen ratio in the Water that Formed the Yellowknife Bay Mudstones in Gale Crater", LPSC abstract 2014. [24] Mousis O. et al. IPPW 2013 Saturn poster [25] Webster C.R. et al., *Appl. Opt.* **29**, 907-917, (1990).

Acknowledgments: Part of the research described here was carried out at the Jet Propulsion Laboratory, California Institute of Technology, under a contract with the National Aeronautics and Space Administration (NASA).